PRODUCTION OF TITANIUM DIBORIDE-REINFORCED NiAl/Ni_3Al MATERIALS BY SPS PROCESS

HYJEK Paweł[1], SULIMA Iwona[1], PAŁKA Paweł[2], JAWORSKA Lucyna[1]

[1] *Pedagogical University, Institute of Technology, Cracow, Poland, EU, phyjek@up.krakow.pl*
[2] *AGH University of Science and Technology, Faculty of Non-Ferrous Metals, Cracow, Poland, EU*

Abstract

In this paper, the effects of various production parameters on the microstructure, mechanical and tribological properties of TiB_2-reinforced NiAl/Ni_3Al intermetallic compound were investigated. The experimental results showed the possibility of producing sintered composites of NiAl/Ni_3Al with 4 vol.% TiB_2 by Spark Plasma Sintering. It was shown that satisfactory results had already been obtained during sintering at 1150 °C and a pressure of 16 MPa. The composites had a nearly theoretical density after sintering already at 1150 °C for 10 min. under pressure of 48 MPa. Applying these parameters also caused achieving the largest Young's modulus (ultrasonic test) and hardness (HV1). Optical microscopy, scanning electron microscopy and X-ray diffraction analysis were used to characterize produced samples. The distribution of alloying elements within intermetallic compound was determined by EDS. TiB_2 reinforcing particles were evenly distributed in the matrix. Tribological tests were made by ball on disc process. The friction coefficient and wear rate of the composites were measured.

Keywords: NiAl/Ni_3Al composites, TiB_2 reinforcing particles, tribological studies, spark plasma sintering

1. INTRODUCTION

For many years alloys based on an intermetallic phase of nickel and aluminum (NiAl, Ni_3Al) have been considered very promising materials for industrial applications. The primary applications for such alloys are in the aerospace industry (mainly for turbine blades), automotive industry (parts of turbochargers, valves, valve seats and cylinder liners operating in internal combustion engines) and manufacturing industry (rollers for furnaces, dies and tools for plastic forming, fixtures of furnaces for thermochemical treatment) [1-5]. The diversity of applications is mainly dictated by the favourable properties of these alloys, such as a low density, high melting point, good oxidation resistance and high strength. For many years studies have also been conducted to improve the properties of materials based on a nickel-aluminum phase, since most of the problems are due to various imperfections of this phase, particularly its high brittleness at room temperature and low ductility [5-7].

Among many available solutions to further raise the mechanical properties of NiAl alloys, the choice of a proper manufacturing method is often quoted, including the use of alloying additions [8-10], reinforcement with the second phase [11-13], producing single crystals [14], or grain refinement. It has been shown that the use of powder metallurgy to produce the NiAl phase can improve its mechanical properties [15-18]. Among the wide spectrum of the methods of powder metallurgy, to mention only free sintering, HP, HP-HT, selective laser sintering (SLS), or microwave sintering, particular attention deserves the new technique of FAST/SPS. It involves sintering of powders under the simultaneous effect of pressure and current. Powders are placed in a die (usually made of graphite) and heating is carried out by passing an electric current (normally pulsed DC) through both the die and the sample (if it is conductive), applying at the same time pressure to the powder. In some respects, the SPS process is similar to hot pressing, but it is characterized by higher heating rate and lower current consumption [19]. In SPS, changes in the microstructure depend to a large extent on the applied parameters of the sintering process. As recommended in [20, 21], to obtain high-quality sintered product, the manufacturing process should involve the following steps: powder activation and refining, formation and growth

of necks, fast compaction and compaction as a result of plastic deformation. The FAST/SPS sintering process along with its flowchart is described in more detail in [22].

Application of this sintering method to alloys based on the intermetallic phase of NiAl can improve the physical and mechanical properties of the resultant materials. The method has already been used with some success in the manufacture of steel [23] and ceramics [24]. The use of a mixture of powders by the authors of this study has enabled making a composite material based on a two-phase NiAl/Ni_3Al matrix reinforced with TiB_2 introduced in an amount of 4 vol.%. Sinters of this type were already produced with very encouraging results by the method of high-pressure high-temperature sintering (HP-HT) [25]. The fabrication of a two-phase structure improves the mechanical and plastic properties [26, 27], while the introduction of a ceramic reinforcing phase helps to upgrade the compatibility and corrosion resistance [28, 29], and occasionally also the tribological properties [7, 30].

The aim of the present study was to determine the parameters of the sintering process (pressure and temperature), which enable producing a relatively high degree of sintering. The choice of the optimum temperature and pressure was based on literature data, which set these parameters for various methods of the composite manufacture [31-33]. In most cases, the sintering temperature of the NiAl matrix materials considered optimal by the authors was comprised in the range of 1100 - 1200 °C.

2. EXPERIMENTAL

Two types of powders were used in the tests, i.e. the Ni79Al21alloy powder (Goodfellow, 45 - 150 μm grain size) and TiB_2 powder (H.C.Starck, 2.5 - 3.5 μm grain size). The powder particle morphology is shown in **Figure 1**. From the technically pure elemental powders, proper blends were prepared capable of producing a composite with 4 vol.% TiB_2 content.

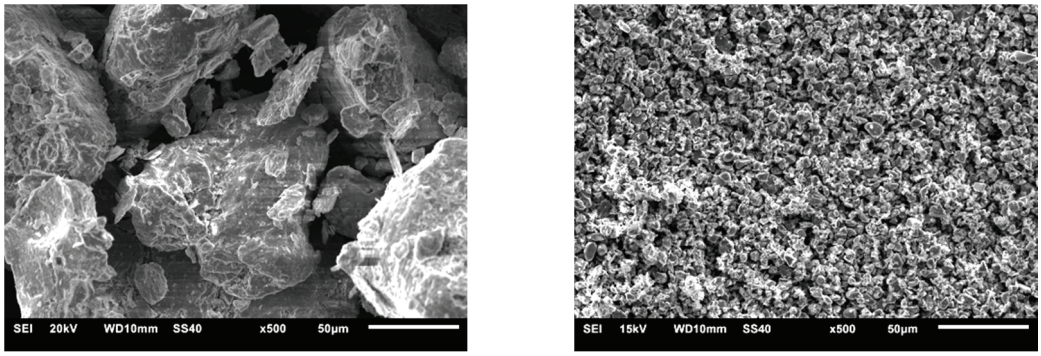

Figure 1 The powder morphology: a) Ni79Al21, b) TiB_2

The powders were mixed for 20 hours in a Turbula type device. Then a batch of powder was sintered by FAST/SPS. The sintering parameters and sample designations are listed in **Table 1**. Heating in the SPS process is obtained by passing a pulsed electric current through the graphite die and reaction mixture. Between the particles of the mixed materials, some sparks are generated, which remove the absorbed gases and oxides, and thus facilitate the formation of active contacts. It has been proved in [34] that compared to the conventional methods, the use of the SPS technique shortens the time and reduces the temperature of the sintering process. It is also possible to control the grain growth and raise the resistance to crack formation. To produce sintered samples, the compaction pressure of 16 and 48 MPa was applied. The process was carried out in an argon atmosphere at a temperature comprised in the range of 1100 - 1200 °C. **Figure 2** shows a schematic diagram of the process recorded for the sample sintered at a temperature of 1100 °C and a pressure of 16 MPa (sample A), and for the sample sintered at a temperature of 1200 °C and a pressure of 48 MPa (sample D). The time of sintering was 10 minutes. The dimensions of the obtained sinters were 5 mm height by 20 mm diameter.

Table 1 The sintering parameters of the Ni-Al alloys reinforced with 4 vol.% TiB_2

Composite	Temperature (°C)	Pressure (MPa)	Sintering time (s)	Poisson`s ratio
A	1100	16	600	0.35
B	1150	16		0.36
C	1150	48		0.36
D	1200	48		0.36

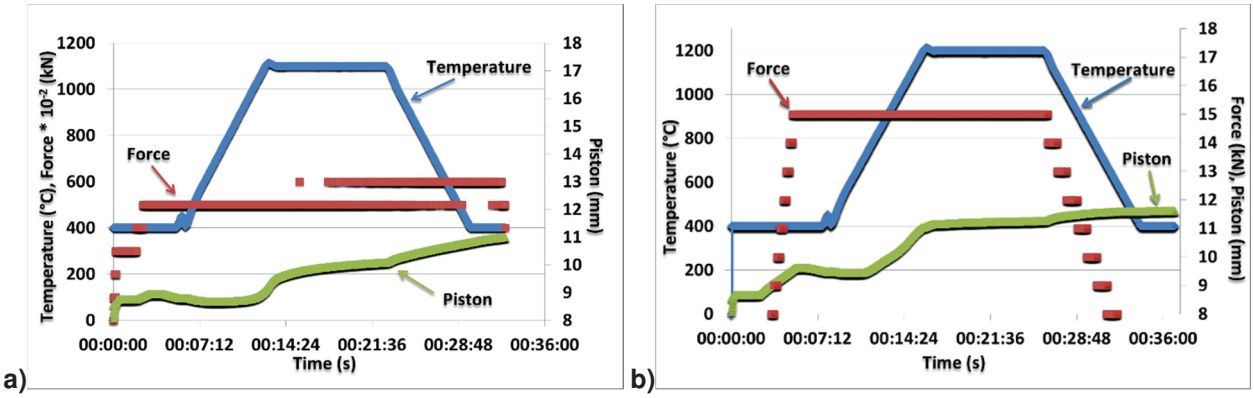

Figure 2 Flowchart of the SPS sintering process carried out on a) samples A and b) samples D

After proper surface treatment, the density and porosity were examined by a hydrostatic method. Young's modulus was determined by the Panametrics Epoch III ultrasonic flaw detector. Vickers hardness HV1 was measured with a NEXUS 4000 hardness tester. Phase identification was performed by X-ray diffraction technique (XRD) using Cu Kα scintillation detector (Bruker D8 Discover). As a next step, the microstructure of the obtained sinters was examined, using for this purpose an Olympus GX-51 optical microscope and a JEOL JSM 6460 LV scanning electron microscope. The parameters analyzed included the homogeneity of the TiB_2 particles distribution in matrix, particle size, and the shape and homogeneity of phases.

Abrasive wear resistance of the produced materials was tested. The tests were conducted in accordance with ASTM G99-05 using a universal ELBIT material tester. The test parameters are compared in **Table 2**.

Table 2 Test parameters of the ball-on-disc

Load applied, *F* (N)	Radius of the wear track, *R* (mm)	Ball (Al_2O_3) diameter, *r* (inch)	Velocity, *v* (m/s)	Test duration, *t* (s)	Temperature *T* (°C)	Environment
5	5	1/8”	0.1	2000	23 ± 2	Air

The coefficients of friction and the depth of furrows (the degree of wear) were automatically measured and recorded in real time by a computer system of the tribotester.

3. RESULTS AND ANALYSIS

Even simple visual assessment of the sinter of the first type (sample A), as well as the light microscopy (**Figure 3a**) and scanning electron microscopy (**Figure 5 a**) conducted next have shown that the material sintered under these conditions is characterized by high porosity. Further studies of the obtained material

showed a low density of 5.98 g/cm^3, i.e. approximately 91 % of the theoretical density, low Young's modulus value of 92 GPa, and a relatively low hardness of 248 HV1. The reason was poor consolidation of the composite material. Raising only one of the manufacturing parameters, i.e. temperature by 50 °C, produced the sinter which, at the same pressure, was characterized by a compact structure and low porosity. Other properties were also improved. The density was now 6.42 g/cm^3, i.e. approximately 98 % of the theoretical density, with Young's modulus and hardness going up to 137 GPa and 479 HV1, respectively. Similar results were obtained in the composites produced at a temperature of 1150 °C and a pressure of 48 MPa, and at a temperature of 1200 °C and a pressure of 48 MPa. The measured values of the density of the sintered materials are shown in **Figure 4 a)**, while **Figure 4 b)** shows the results obtained for the hardness and Young's modulus.

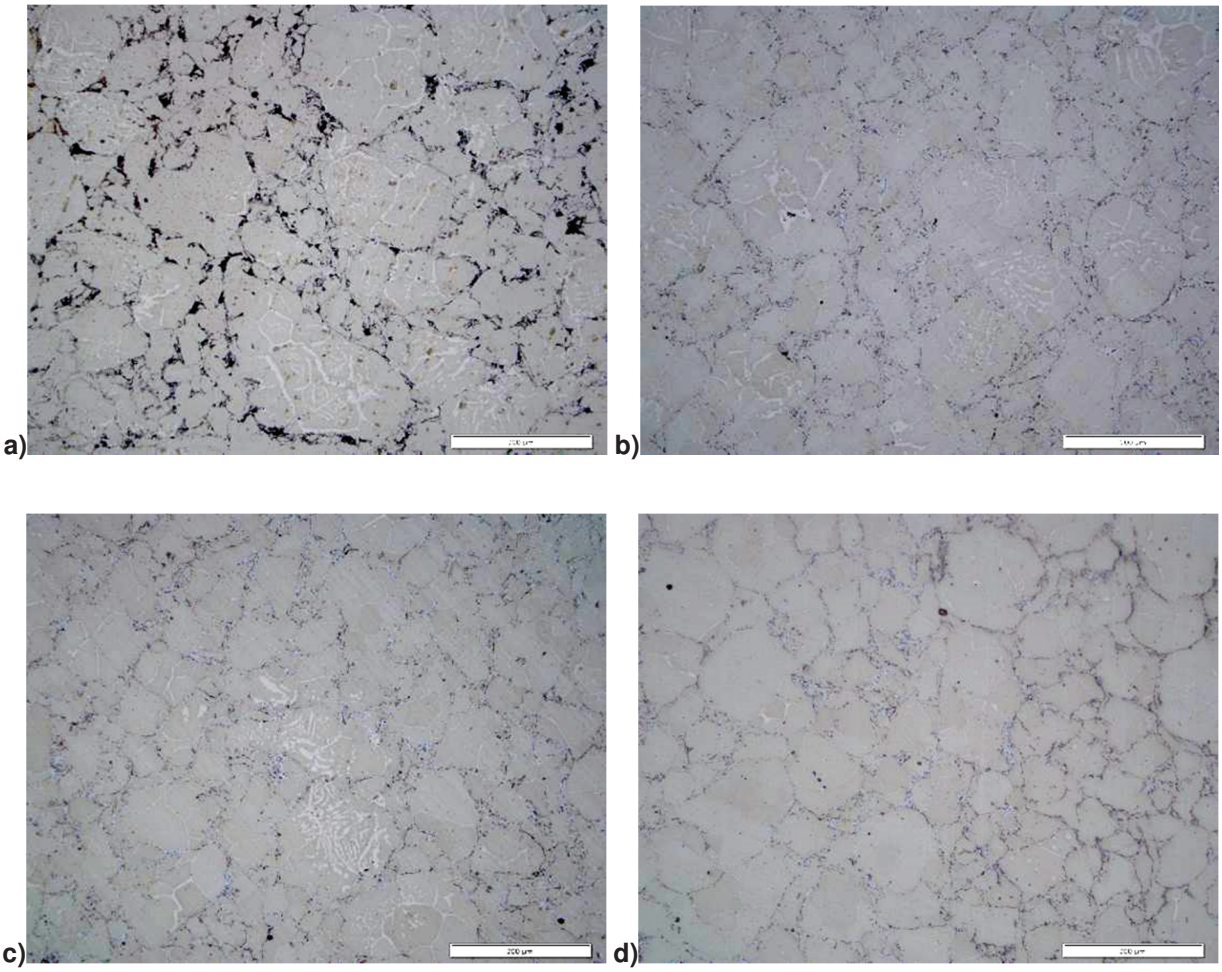

Figure 3 Microstructure of the NiAl/Ni_3Al + 4 vol.% TiB_2 sample sintered under different parameters of temperature and pressure: a) type A, b) type B, c) type C, d) type D - optical microscope

All sintered samples were characterized by a relatively uniform distribution of the TiB_2 particles (**Figures 3, 5 and 6**). The matrix had a fairly complex structure composed of two distinct phases, where in areas darker (the average content of aluminum and nickel corresponding to the NiAl phase), there was a bright area (the average content of Al and Ni corresponding to the Ni_3Al phase) distributed in an uneven and random manner, but occasionally forming a sort of sub-boundaries. Microhardness measurements taken in these areas of the matrix showed variations in the results, depending on how advanced the studies of these areas (indentations) were.

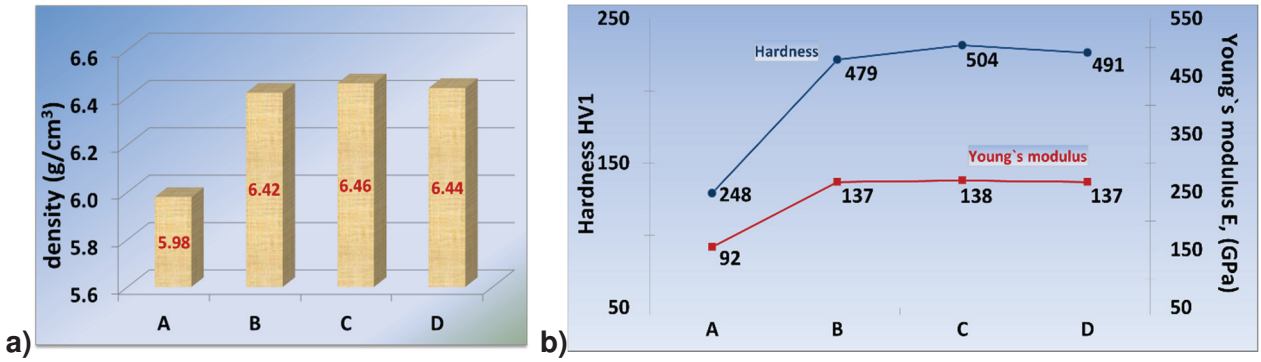

Figure 4 Change of: a) density and b) hardness and Young's modulus values obtained for the NiAl/Ni_3Al + 4 vol.% TiB_2 sample sintered under different parameters of temperature and pressure

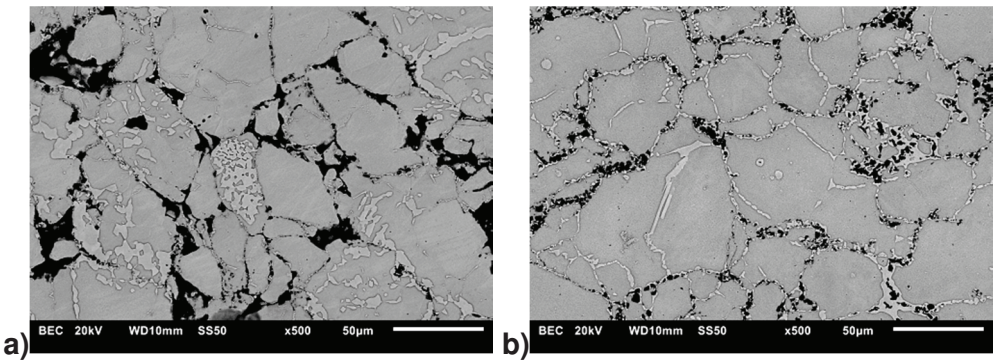

Figure 5 Microstructure of the NiAl/Ni_3Al + 4 vol.% TiB_2 composites sintered at a pressure of 16 MPa: a) type A, b) type B

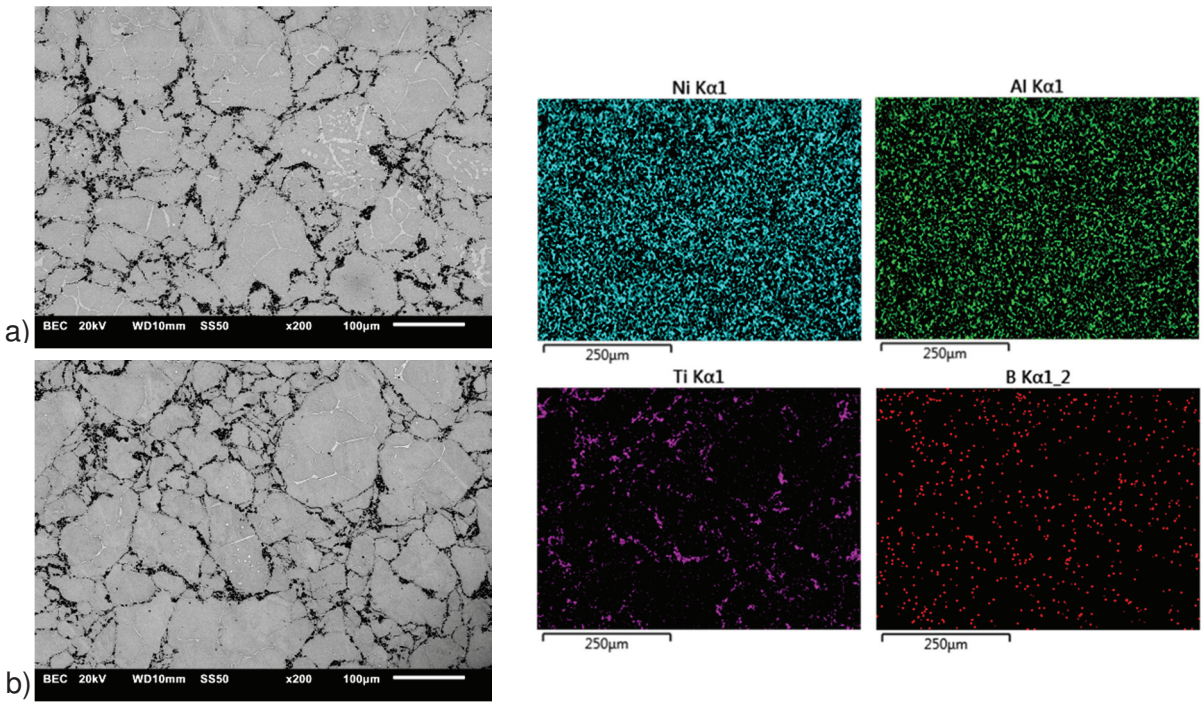

Figure 6 Microstructure of the NiAl/Ni_3Al + 4 vol.% TiB_2 sample sintered at a pressure of 48 MPa, a) sample C, b) sample D - map showing the distribution of individual phases

The X-ray analysis revealed in the sintered materials the presence of the three phases of NiAl, Ni_3Al and TiB_2. The results of the XRD analysis made for the extreme sintering parameters (samples A and D) are shown in **Figure 7**.

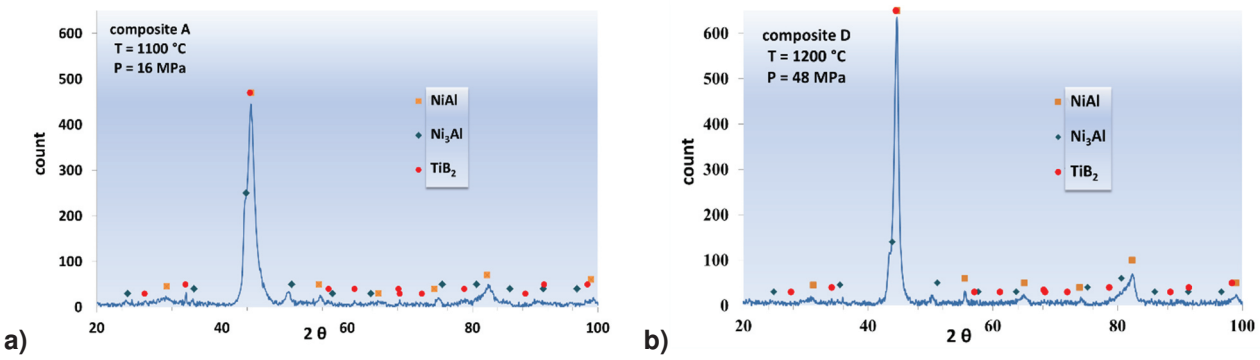

Figure 7 The results of X-ray analysis of the sintered NiAl/Ni_3Al + 4 vol.% TiB_2 compound

Analysis of the results (**Figure 8**) obtained in the ball-on-disc abrasion test has led to the conclusion that sinters of type A are characterized by the highest coefficient of friction and the greatest depth of wear (loss of material).

The coefficients of friction and the depth of wear in the remaining groups are at a similar level. It seems, however, that the highest resistance to wear has the D-type composite made at a temperature of 1200 °C and a pressure of 48 MPa. The coefficients of friction are for this composite comprised in the range of 0.3 - 0.35, while for composites B and C they are comprised in the range of 0.35 - 0.4.

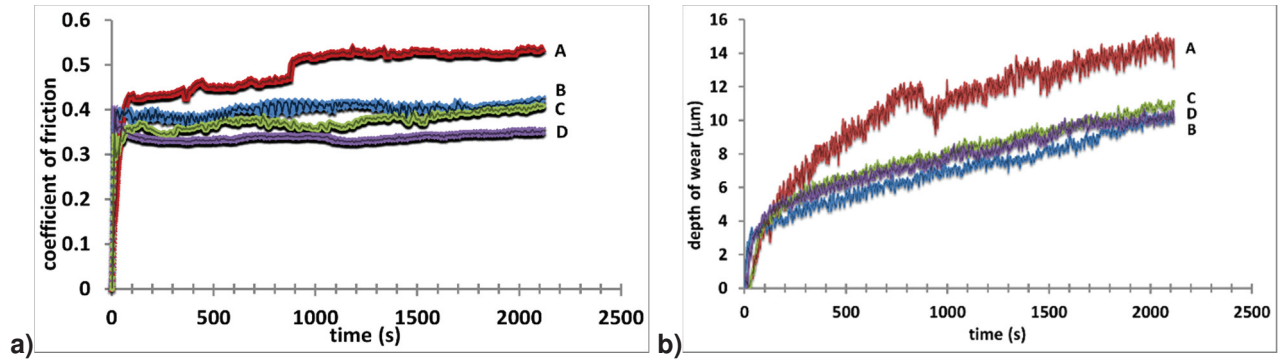

Figure 8 a) Coefficients of friction and b) depths of wear, obtained for the NiAl/Ni_3Al + 4 vol.% TiB_2 samples sintered under different parameters of temperature and pressure

Careful examination of the wear traces left by the conducted process has revealed more details about the wear mechanism prevailing in the sintered NiAl/Ni_3Al + 4 vol.% TiB_2 under given conditions of the ball-on-disc test. Scratches, TiB_2 particles knocked out of their original location, fragments of material torn out (black holes), seizure (containing both TiB_2 and matrix particles unevenly displaced) were reported to occur (**Figures 9-11**). In the areas of seizure, the presence of oxygen was additionally traced. Probably it has originated from oxides formed during the process of friction or penetrating into the material from the test ball made of Al_2O_3. Examinations of the ball under a microscope did not show any traces of wear. Also the weight of the ball after the friction test did not differ much from the original weight (it was comprised within the margin of error). In addition to the TiB_2 particles knocked out and traces of seizure observed on them, also defragmentation of these hard and brittle particles was noted (**Figure 10**). Rapid wear of the composite made at the lowest temperature and pressure parameters (sample A) is probably due to the TiB_2 particles loosely embedded in

the grain boundaries, which allows their easy and fast knocking out, combined with the formation of numerous active bodies that cause furrows and cracks.

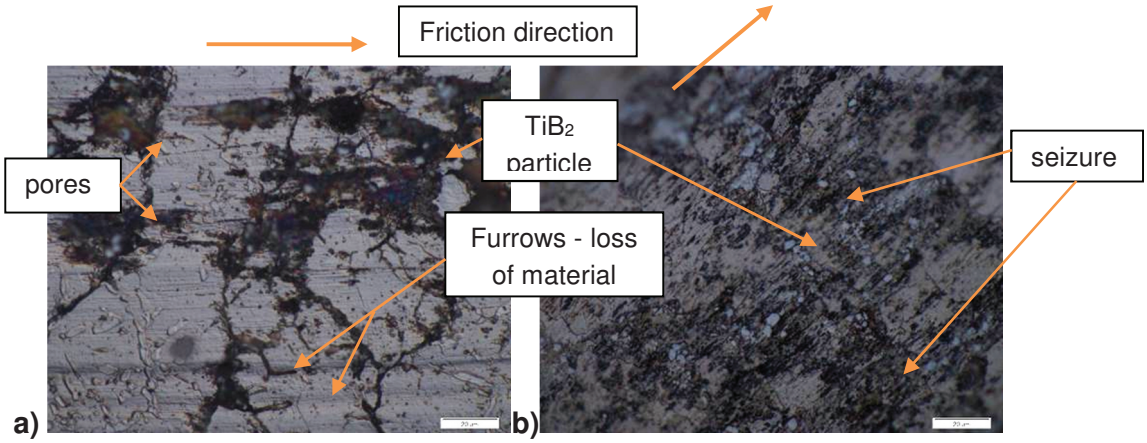

Figure 9 Microstructure of composite: a) A and b) C after the process of friction; optical microscope

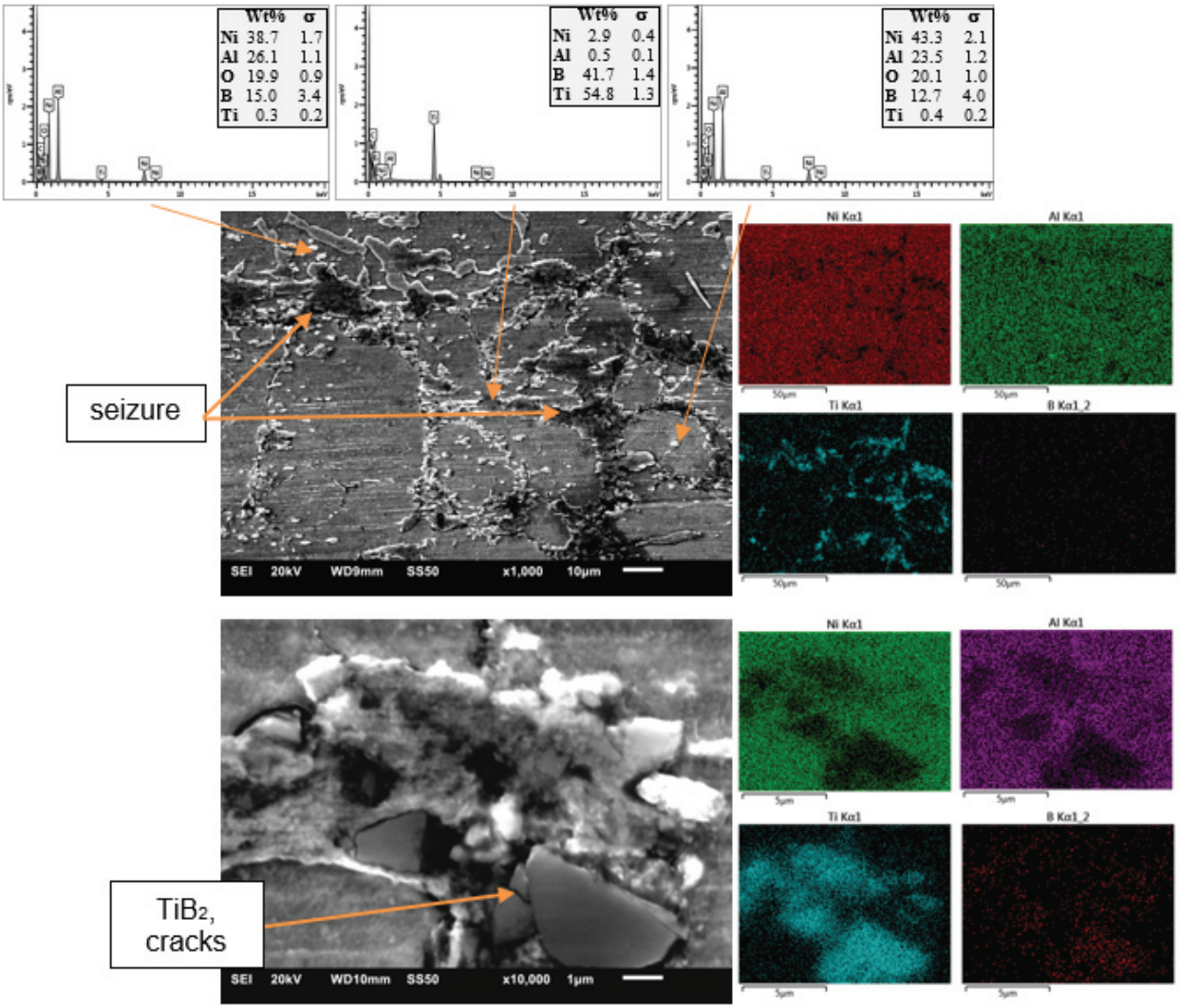

Figure 10 Microstructure and EDS analysis of composite A after the process of friction

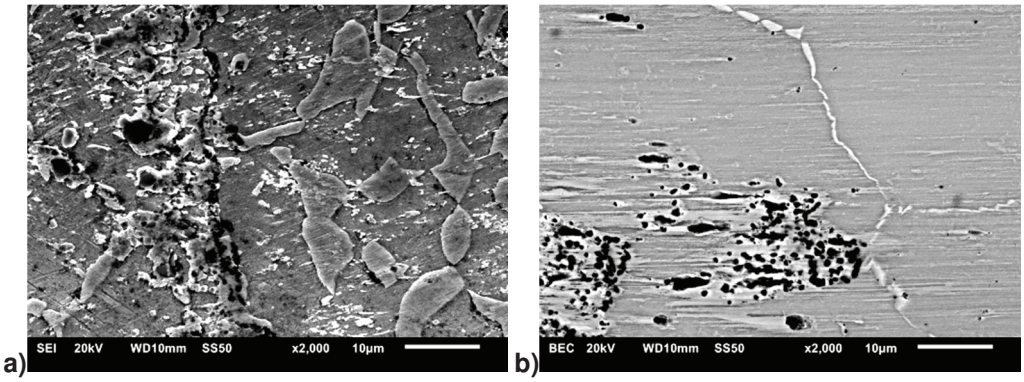

Figure 11 Microstructure and EDS analysis of composite: a) B and b) D after the process of friction

4. CONCLUSIONS

As a result of studies of the physical, mechanical and tribological properties, combined with microstructure examinations, it has been concluded that the selected parameters of pressure and temperature enable producing the NiAl/Ni_3Al + 4 vol.% TiB_2 composite by FAST/SPS.

The manufactured composites (B, C, D) are characterized by a structure with minimal porosity. The characteristic values obtained for the sintered composites are: the density of 6.44 g/cm^3, the Young's modulus of 137 GPa, and Vickers hardness of 490 HV1.

Measurements of the Vickers hardness have shown significant differences in the values of this parameter occurring within one sample, involving a great variety of the phases of different distribution present in the composite.

ACKNOWLEDGEMENTS

This work was carried out with financial support through statutory funds of Pedagogical University in Cracow. Apparatus co-financed by the European Regional Development Fund under the Infrastructure and Environment Programme: "For the Development of the Infrastructure and environment".

REFERENCES

[1] SIKKA, V. K., DEEVI, S. C., VISWANATHAN, S., SWINDEMAN, R. W., SANTELLA, M. L. Advances in processing of Ni_3Al-based intermetallics and applications. *Intermetallics*, 2000, vol. 8, pp. 1329-1337.

[2] DEEVI, S. C., SIKKA, V. K. Nickel and iron aluminides: an overview on properties, processing, and applications. *Intermetalics*, 1996, vol. 4, pp. 357-375.

[3] MIRACLE, D. B., DAROLIA, R. NiAl and its alloys. I*ntermetallic Compounds. Structural Applications of Intermetallic Compounds.* Ed. Westbrook J. H. and Fleischer R. L., 1995. 346 p.

[4] NOEBE, R. D., WALSON, W. S. Prospects for development of structural NiAl alloys. *Structural Intermetallics,* 1997, pp. 573-584

[5] STOLOFF, N. S, LIU, C. T, DEEVI, S. C. Emerging applications of intermetallics. *Intermetallics*, 2000, vol. 8, pp. 1313-1320.

[6] DAROLIA, R., WALSTON, W.S. Development and characterization of high strength NiAl single crystal alloys. In *First Inter. Symp. on Structural Intermetallics*, TMS, Warrendale, PA, 1997, pp. 585-594

[7] STOLOFF, N. S., SIKKA, V. K. *Physical Metallurgy and Processing of Intermetallic Compounds*. New York, Chapman & Hall, 1996. 684 p.

[8] KOVALEV, A. I., BARSKAYA, R. A., WAINSTEIN, D .L. Effect of alloying on electronic structure, strength and ductility characteristics of nickel aluminide. In *Proceedings of the 7th Int. Conference on Nanometer-Scale Science and Technology and the 21st European Conference on Surface Science*, 2003, vol. 532-535, pp. 35-40.

[9] JOHNSON, D. R., OLIVER, B. F., NOEBE, R. D., WHITTENBERGER, J. D. NiAl-based polyphase in situ composites in the NiAl-Ta-X (X = Cr, Mo, or V) systems. *Intermetallics*, 1995, vol. 3, pp. 493-503.

[10] JOHNSON, D. R. Processing and Mechanical Properties of NiAl-Based In-Situ Composites. *NASA Contractor Report 195333*, 1995, 204 p.

[11] ALMAN, D. E., STOLOFF, N. S. Powder fabrication of monolithic and composite NiAl. *International Journal of Powder Metallurgy*, 1991, vol. 27, pp. 29-41.

[12] FRAŚ, E., JANAS, A., KURTYKA, P., WIERZBIŃSKI, S. Structure and properties of cast Ni_3Al/TiC and Ni_3Al/TiB_2 composites. Part II. Investigation of mechanical and tribological properties and of corrosion resistance of composites based on intermetallic phase Ni_3Al reinforced with particles of TiC and TiB_2. *Arch Metall Mater*, 2004, vol. 49, pp. 113-141.

[13] SAUTHOFF, G. Multiphase intermetallic alloys for structural applications. *Intermetallics*, 2000, vol. 8, pp. 1101-1109.

[14] DAROLIA, R., WALSTON, W., NOEBE, R., GARG, A., OLIVER, B. Mechanical properties of high purity single crystal NiAl. *Intermetallics*, 1999, vol. 49, pp. 1195-1202.

[15] CHOUDRY, M.S., DOLLAR, M., EASTMAN, J.A. Nanocrystalline NiAl-processing, characterization and mechanical properties. *Materials Science and Engineering: A*, 1998, vol. 256, pp. 25-33.

[16] KOCH, C.C. Intermetallic matrix composites prepared by mechanical alloying-a review. *Materials Science and Engineering: A*, 1998, vol. 244, pp. 39-48.

[17] IVANOV, E., GRIGORIEVA, T., GOLUBKOVA, G. BOLDYREV, V. et al. Synthesis of nickel aluminides by mechanical alloying. *Mater Lett*, 1988, vol. 7, pp. 51-54.

[18] YANG, J. M., KAO, W. H., LIU, C. T. Development of Nickel aluminide matrix composites. *Materials Science and Engineering: A*, 1989, vol. 107, pp. 81-91.

[19] MUNIR, Z. A., ANSELMI-TAMBURINI, U., OHYANAGI, M. The effect of electric field and pressure on the synthesis and consolidation of materials: A review of the spark plasma sintering method. *J. Mater Sci*, 2006, vol. 41, pp. 763-777.

[20] TOKITA, M. Mechanism of spark plasma sintering. In *Proceedings of NEDO International Symp. on Functionally Graded Materials*, 1999, vol. 22, pp. 1-13.

[21] ZHAOHUIA, Z., FUCHIA, W., LINA, W. SHUKUIA, L., OSAMUB, S. Sintering mechanism of large-scale ultrafine-grained copper prepared by SPS method. *Materials Letters*, 2008, vol. 62, pp. 3987-3990.

[22] SULIMA, I. Consolidation of AISI 316L austenitic steel - TiB_2 composites by SPS and HP-HT technology. Sintering Techniques of Materials, In*Tech-Open Access Publisher*, 2015, no. 7, pp. 125-153.

[23] SULIMA, I., PUTYRA, P., HYJEK, P., TOKARSKI, T. Effect of SPS parameters on densification and properties of steel matrix composites. *Advanced Powder Technology*, 2015, no. 26, pp. 1152-1161.

[24] KLIMCZYK, P. et al. Al_2O_3-cBN composites sintered by SPS and HPHT methods. *Journal of the European Ceramic Society*, 2016, vol. 36, pp. 1783-1789.

[25] HYJEK, P., SULIMA, I., FIGIEL, P. NiAl composite reinforced with TiB2 ceramic particles. *Innovative Manufacturing Technology, 2013*, IZW Krakow, 2013, pp. 31-42.

[26] NOEBE, R. D., MISRA A., GIBALA, R. Plastic flow and fracture of B2 NiAl-based intermetallic alloys containing a ductile second phase. *ISIJ International*, 1991, vol. 31, pp. 1172-1185.

[27] INOUE, A., MASUMOTO, T., TOMIOKA, H. , Microstructure and mechanical properties of rapidly quenched $L2_0$ and $L2_0$+$L1_2$ alloys in Ni-Al-Fe and Ni-Al-Co systems. *Journal of Materials Science*, 1984, vol. 19, pp. 3097-3106.

[28] MISRA A. K. Theoretical analysis of compatibility of several reinforcement materials with NiAl and FeAl matrices. *NASA Contractor Report 182291*, 1989, 21 p.

[29] GAO, W., LI, Z. *Developments in high-temperature corrosion and protection of materials*. Woodhead Publishing, 2008. 672 p.

[30] HAWK, J. A., ALMAN, D. E. Abrasive wear behaviour of NiAl and NiAl-TiB_2 composites. *Wear*, 1999, vol. 225-229, pp. 544-556.

[31] MICHALSKI, A., JAROSZEWICZ, J., ROSIŃSKI, M., SIEMIASZKO, D. NiAl-Al_2O_3 composites produced by pulse plasma sintering with the participation of the SHS reaction. *Intermetallics*, 2006, vol. 14, pp. 603-606.

[32] UDHAYABANUA, V., RAVIA, K. R., MURTY, B. S. Development of in situ NiAl-Al_2O_3 nanocomposite by reactive milling and spark plasma sintering. *Journal of Alloys and Compounds*, 2011, vol. 509, pp. S223-S228.

[33] XIAO, Y., SHI, X., ZHAI, W., YAO, J., XU, Z., CHEN, L., ZHU, Q. Tribological performance of NiAl self-lubricating matrix composite with addition of graphene at different loads. *Journal of JMEP,* 2015, vol. 24, pp. 2866-2874.

[34] FIGIEL, P., ROZMUS, M., SMUK, B. Properties of alumina ceramics obtained by conventional and nonconventional methods for sintering ceramics. *J. of Achievements in Mat. and Manuf. Engineering*, 2011, vol. 48, pp. 29-34.